

A hierarchical climatic zoning method for energy efficient building design applied in the region with diverse climate characteristics

Article

Accepted Version

Creative Commons: Attribution-Noncommercial-No Derivative Works 4.0

Xiong, J., Yao, R. ORCID: <https://orcid.org/0000-0003-4269-7224>, Grimmond, S. ORCID: <https://orcid.org/0000-0002-3166-9415>, Zhang, Q. and Li, B. (2019) A hierarchical climatic zoning method for energy efficient building design applied in the region with diverse climate characteristics. *Energy and Buildings*, 186 (2019). pp. 355-367. ISSN 0378-7788 doi: <https://doi.org/10.1016/j.enbuild.2019.01.005> Available at <https://centaur.reading.ac.uk/82112/>

It is advisable to refer to the publisher's version if you intend to cite from the work. See [Guidance on citing](#).

To link to this article DOI: <http://dx.doi.org/10.1016/j.enbuild.2019.01.005>

Publisher: Elsevier

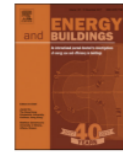
All outputs in CentAUR are protected by Intellectual Property Rights law, including copyright law. Copyright and IPR is retained by the creators or other copyright holders. Terms and conditions for use of this material are defined in the [End User Agreement](#).

www.reading.ac.uk/centaur

CentAUR

Central Archive at the University of Reading

Reading's research outputs online



A hierarchical climatic zoning method for energy efficient building design applied in the region with diverse climate characteristics



Jie Xiong^{a,c,d}, Runming Yao^{a,c,*}, Sue Grimmond^d, Qiulei Zhang^{a,b}, Baizhan Li^{a,b,*}

^aJoint International Research Laboratory of Green Buildings and Built Environments (Ministry of Education), Chongqing University, Chongqing 400045, China

^bNational Centre for International Research of Low-carbon and Green Buildings (Ministry of Science and Technology), Chongqing University, Chongqing 400045, China

^cSchool of the Built Environment, University of Reading, Reading RG6 6DF, UK

^dDepartment of Meteorology, University of Reading, Reading RG6 6BB, UK

A hierarchical climatic zoning method for energy efficient building design applied in the region with diverse climate characteristics

Jie Xiong^{1,3,4}, Runming Yao^{1,3*}, Sue Grimmond⁴, Qiulei Zhang^{1,2}, Baizhan Li^{1,2*}

¹ Joint International Research Laboratory of Green Buildings and Built Environments (Ministry of Education), Chongqing University, Chongqing 400045, China

² National Centre for International Research of Low-carbon and Green Buildings (Ministry of Science and Technology), Chongqing University, Chongqing 400045, China

³ School of the Built Environment, University of Reading, Reading RG6 6DF, UK

⁴ Department of Meteorology, University of Reading, Reading RG6 6BB, UK

*Corresponding author: r.yao@reading.ac.uk; baizhanli@cqu.edu.cn

Abstract

The climate-responsive strategies for energy efficient building design and management require a detailed understanding of the local climatic conditions, while climate zones are fundamental to building regulations and the application of technologies. Smaller and more homogeneous climate zones could help policy-makers and building designers to improve building energy efficiency while improving the indoor thermal environment. A new climate zoning method, with two-tier

21 classification designed for passive building design, is proposed, using climate data (degree-days,
22 relative humidity, solar radiation and wind speed) with Hierarchical Agglomerative Clustering
23 (HAC) following the Ward's method. The method is applied to the *Hot Summer and Cold Winter*
24 (*HSCW*) zone of China as a showcase, where there are no fine climate zones for energy efficient
25 building design with diverse climate characteristics. Seven sub-zones that consider both cooling and
26 heating demands are generated in Tier 1. In the second tier, the HSCW zone is further sub-divided
27 into three humidity groups, three solar radiation clusters, and four wind speed clusters. To assess the
28 impact of climate zoning on building heating and cooling, EnergyPlus simulations are conducted
29 with the output of heating and cooling load. The cooling loads decrease from sub-zone A to B to C
30 (mean = 82.8, 65.3, 43.8 kWh m⁻², respectively) with sub-zone mean heating A1 larger than A2 and
31 A3, B1 larger than B2, and C1 larger than C2, which is in accordance with the assumption made in
32 the first-tier division. The higher wind speeds can raise the possibility of natural ventilation, and
33 further increase the free-running period (FRP) when heating and cooling are not needed. The
34 proposed zones are mapped and provide a useful reference for the policy/building code makers for
35 heating and cooling strategies in this region. The method to create the climate zones could be
36 applied in any region with local climate data.

37
38 **Keywords:** Climatic zoning; Energy efficient building design; Hierarchical Agglomerative
39 Clustering (HAC); Passive design; Hot Summer and Cold Winter (HSCW) zone

41 **Highlights**

- 42 • New climate zoning method to help improve building energy designs
- 43 • Method applicable to diverse climates and will enhance natural resource utilisation
- 44 • Method demonstrated in the HSCW zone of China
- 45 • Hierarchical Agglomerative Clustering using 166 weather stations (10 years)
- 46 • New HSCW sub-zones allow improved spatial resolution of heating/cooling loads

47

48 **Acronyms**

<i>CDD</i>	Cooling Degree-Days
<i>HAC</i>	Hierarchical Agglomerative Clustering
<i>HDD</i>	Heating Degree-Days
<i>HSCW</i>	Hot Summer and Cold Winter zone
<i>HVAC</i>	Heating, Ventilation and Air-Conditioning
<i>IQR</i>	Inter-quartile range
<i>R_a</i>	Incoming solar radiation
<i>RH</i>	Relative humidity
<i>WS</i>	Wind speed

49

50 **Nomenclature**

<i>CDD26</i>	Cooling Degree-Days (base = 26 °C) (°C)
$C_z \frac{dT_z}{dt}$	Energy stored in zone air (W)
<i>D</i>	Squared Euclidean distance of a variable
$d_{T \leq 5}$	Number of days daily mean temperature ≤ 5 °C
$d_{T \geq 25}$	Number of days daily mean temperature ≥ 25 °C
<i>HDD18</i>	Heating Degree-Days (base =18 °C) (°C)
$\dot{m}_{inf} C_p (T_{\infty} - T_z)$	Heat transfer due to infiltration of outside air
<i>n</i>	Total number of stations in each cluster
\dot{Q}_{sys}	The output from mechanical systems (W)
<i>T_{av}</i>	Monthly mean air temperature (°C)
<i>T_{av, max}</i>	Monthly mean of daily maximum air temperature (°C)
<i>T_i</i>	Daily average temperature (°C)
<i>T_{B,C}</i>	Base temperature for CDD (=26 °C)

$T_{B,H}$	Base temperature for HDD (=18 °C)
v	Daily mean of a variable
$\sum_{i=1}^{N_{surfaces}} h_i A_i (T_{si} - T_z)$	Convective heat transfer from the zone surfaces (W)
$\sum_{i=1}^{N_{zones}} \dot{m}_i C_p (T_{zi} - T_z)$	Heat transfer due to inter-zone air mixing (W)
$\sum_{i=1}^{N_{sl}} \dot{Q}_i$	Total convective internal load (W)

Subscripts

i, j, k	The identity of a station (or a cluster)
(ij)	The identity of a new cluster formed from two existing stations (or clusters)
$ij, ik, jk, (ij)k$	Connection between two stations (or clusters)
t	Time

51

52 **1 Introduction**

53 As excessive energy consumption contributes to climate change [1,2] and air pollution [3,4],
54 governments from most countries have reached consensus to reduce carbon emissions. At the Paris
55 Conference on Climate Change 2015, China pledged that their CO₂ emissions would peak around
56 2030, and to reduce CO₂ emission by 60-65% of the 2005 level [5]. As buildings account for about
57 40% of European [6] and 27.5% of China [7] total energy consumption, energy efficient building
58 design is paramount if the carbon reduction target is to be met.

59 Passive building design can permit energy efficient and “healthy” architecture design to
60 maximise occupants' comfort and health by harmonizing local climates and site conditions with
61 architectural design and building technologies [8]. The principle is based on climate-responsive
62 strategies taking advantage of natural resources like sunlight and wind while avoiding exposure to
63 heat and cold from the surroundings and excessive radiation, so effective passive design requires a
64 detailed understanding of the local climatic conditions. The adaptability of building energy-

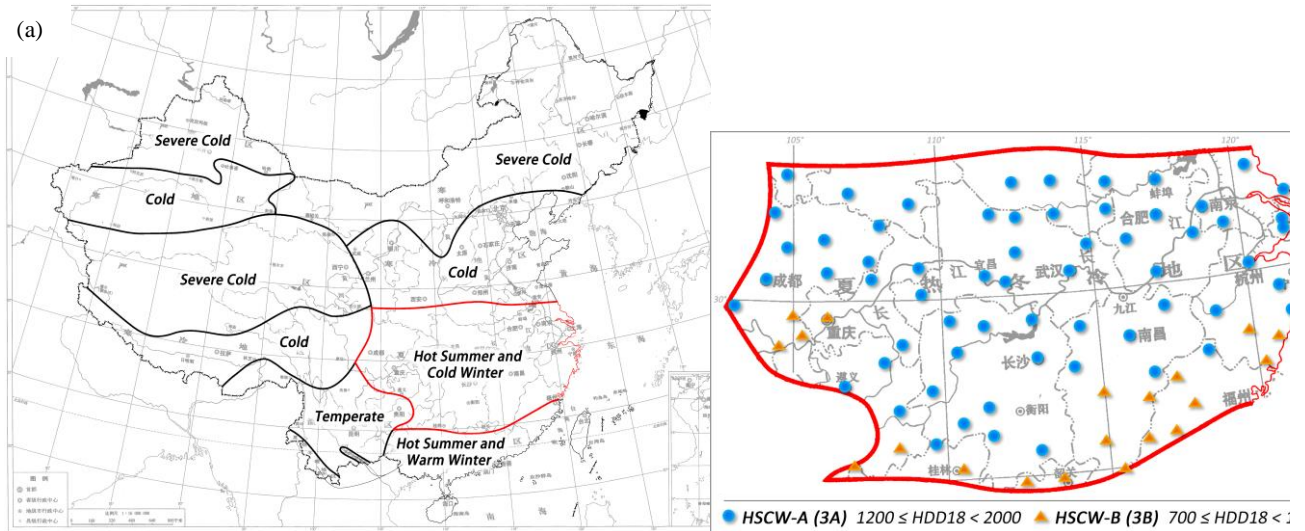
65 efficiency technologies varies with geographic locations [9–14]. Modifying passive technologies,
66 including variations in insulation [15–19], natural ventilation [20–22], shading [23,24] and solar
67 space heating [14,25], can effectively reduce energy demands for heating and cooling of buildings.

68 When establishing energy conservation regulations, it is essential to be aware of local climate
69 characteristics. Climatic zoning allows 1) regulation of some thermal properties of a building (e.g.
70 shape coefficient, U-values (wall, roof, glazing), window to wall ratio); 2) overall energy savings
71 targets of the optimally-designed building compared with a baseline scenario; 3) annual energy
72 consumption quotas. China considered the first two in their current standards when a design scheme
73 cannot meet specific limitations perfectly. The total energy consumption of a design scheme and a
74 baseline scenario were calculated to provide a comparison for decisions [26,27]. France specified
75 the maximum energy consumption per unit floor area for each climate zone in their standard, as part
76 of their near-zero energy building in 2020 target [28].

77 Climate zoning is the preliminary work to establish the building regulations for energy
78 efficiency for most countries. As China's (land area = 9.6 million km²) mainland extends from 21°N
79 to 54°N, and 74°E to 135°E, the climate is diverse: subtropical in the south to the temperate in the
80 north (Figure 1). The Ministry of Housing and Urban-Rural Development of China's (MOHURD)
81 *GB 50176-93 Thermal Design Code for Civil Building* is a national standard to match regional
82 climates with thermal design of buildings whilst ensuring compliance with basic indoor thermal
83 environment requirements. This standard defines five zones based on climatic conditions (Figure
84 1a): Severe Cold (SC), Cold (C), Hot Summer and Cold Winter (HSCW), Hot Summer and Warm
85 Winter (HSWW) and Temperate (T).

86

(b)



87 Figure 1: Climate zones for building thermal design (a) for China and (b) the Hot Summer and Cold Winter
88 zone with cities location (dots) in sub-zones 3A (blue) and 3B (orange) (Modified from [29,30])

89

90 Improved energy efficiency policies can be obtained from more detailed zoning. For example
91 in the USA at the national level, zoning is by state based on thermal (0-8) and moisture (Moist, Dry
92 and Marine) conditions creating 19 climate zones [31]. To provide more guidance the California
93 Energy Commission uses 16 zones derived primarily from 600 weather stations mean summer and
94 winter temperatures [32,33]. Australia's 8 climate zones [34] are divided by the Nationwide House
95 Energy Rating Scheme (NatHERS) into 69 climate zones [35]. The maximum permissible energy
96 loads and energy performance ratings in different climate zones are various [36], allowing
97 comparison of buildings in different weather conditions across Australia.

98 To improve the indoor thermal environment, energy is used for heating and cooling. The
99 amount used varies with climate and living standards. The objective of passive design is to account
100 for the outdoor climate to improve indoor comfort while reducing energy consumption; i.e. extend
101 the free-running period (FRP) when heating and cooling are not used [37]. Given the paucity of
102 studies of climatic dynamics impact on passive design, metrics improved climate zones should
103 enhance: building energy efficiency regulations, indoor thermal comfort and energy efficiency.

104 The objective of this paper is to present a new method to generate climate zones for building
105 energy design. Variables relevant to passive design, including temperature, relative humidity, solar

106 radiation and wind [38] are used. However, for a region with diverse climate characteristics, as
107 more variables are considered, greater spatial heterogeneity becomes evident creating potential
108 problems for operational policy and building code. This work aims to efficiently category this
109 region with climate characteristics from historical observation data. To create homogeneous zones,
110 a two-tier approach is taken: first, thermal properties based on heating degree days (HDD) and
111 cooling degree days (CDD); and second, relative humidity, solar radiation and wind speed variables
112 are used. The latter impact specific passive materials or technologies for design. The method is
113 applied to the Hot Summer and Cold Winter zone of China as a showcase. The implications of the
114 proposed sub-zones to typical residential building energy needs are assessed.
115

116 **1.1 Climate classification for building design**

117 The success of early climate classifications based on climate response features related to
118 vegetation [39] (e.g. the well-known Köppen system [40,41]) has prompted their use for building
119 energy standards. Olgyay [42] analysed the influence of climate on building design and suggested
120 four main climate types, i.e. cool, temperate, hot and arid, and hot and humid in the early 1960s.
121 Subsequently, Givoni [38] proposed four major climates, i.e. hot, warm-temperate, cool-temperate
122 and cold, based on the influences of climatic features on human comfort and the thermal
123 performance of buildings. According to the distinct climate characteristics, climate zones have been
124 created using various techniques, including classification [29,31,34,43–50] and clustering
125 [43,51,52], in different regions of the world.

126 Classification uses manual training to create the divisions. Some countries (e.g. China [29],
127 United States [31], Australia [34] and Japan [44]) select variables to characterize the diversity of
128 their climates and then create the climate zones using subjective thresholds. Most commonly mean
129 air temperature (at 1.5 m above ground level) is the primary efficacy variable used for building
130 energy performance climate zones (Table 1) [53]. Often degree-days, defined as the sum of positive
131 differences relative to a base temperature over time [54], are used as an alternative of temperature
132 for the consideration of both heating and cooling needs, and it is most relative to energy

133 consumption due to space heating and cooling [54]. While temperature based metrics cannot reflect
 134 the whole understanding of the climate and its impacts on the building energy consumptions [55], it
 135 was often applied in combination with other climate variables. India’s five-zone classification
 136 considers temperature and relative humidity as two comfort-related factors [45,46]. Although Dash
 137 *et al.* [56] propose seven zones for India based on solar radiation and air temperature, with the
 138 criteria of considering both weather conditions and solar photovoltaic production. The Spanish
 139 Climatic Severity Index (CSI) [57] (as cited in [48]), based on the heating and cooling demands
 140 relative to the same building in a reference location, creates 16 regions from five winter and four
 141 summer climate zones [47]. Furthermore, the CSI is characterised by climatic variables including
 142 degree-days based on 20 °C (HDD20 or CDD20) and sunshine hours relative to the maximum
 143 possible [48,49]. When Verichev and Carpio’s [58] apply the Spanish CSI method to Chile, and
 144 three zones are identified. Morocco has been subdivided using winter degree days and summer
 145 degree days, and 6 climate zones are identified with the aid of simulation results of the annual
 146 heating and cooling requirements of buildings in eleven representative cities [50].

148 Table 1: Variables used in national building standards to identify climate zones include air temperature (T),
 149 monthly mean T (T_{av}), monthly mean of daily max T ($T_{av, max}$), number of days $T_{av} \leq 5$ °C ($d_{T \leq 5}$) or $T_{av} \geq 25$
 150 °C ($d_{T \geq 25}$), cooling/heating degree-days (CDD/HDD) and relative humidity (RH)

Country [ref]	Zone numbers and names	Variables			Considers
		Temperature	DD	Moisture	
China [29, 30]	5: SC, C, HSCW, HSWW, T	T_{av} coldest month T_{av} hottest month $d_{T \leq 5}$ $d_{T \geq 25}$	CDD26 HDD18	---	Building thermal performance in winter and summer
US [31]	19: 9 thermal, 3 moisture	T_{av} Annual T_{av} .	CDD10 HDD18	Annual precipitation	Heating and cooling demands together with moisture
Australia [34]	8	$T_{av, max}$ January T_{av} July	Average annual HDD	Average 3 pm January vapour pressure	Heating demands cooling demands focus on extreme heat
Japan [44]	8	---	HDD18	---	Heating demands only
India [45,46]	5: hot-dry, warm-humid, composite, temperate, cold	T_{av} $T_{av, max}$	---	Mean monthly RH	Extreme of two comfort-related factors
Spain [47–49]	16: Winter: A-E Summer: 1-4	---	---	---	Winter Climatic Severity Index, Summer Climatic Severity Index Data: simulations of buildings of various types
Morocco [50]	6	---	HDD18 CDD21	---	Winter degree days and summer degree days Simulations of annual heating and cooling requirements used as a reference

151

152 Clustering analysis provides a possibility to consider multiple aspects of climate variables
153 simultaneously (like different variables or seasonal difference of the same variables for time-serious
154 data). It is further divided into two approaches, i.e. non-hierarchical (or flat) [59] and hierarchical
155 techniques. An example of the former (K-means) assigns data into a pre-specified number of
156 clusters or groups based on the distance between itself and a cluster centre point using a very
157 efficient algorithm that may only find a local optimum [60]. Hierarchical clustering includes
158 bottom-up (cumulative) and top-down (divisive) approaches. Hierarchical agglomerative clustering
159 (HAC) methods have the advantage of not requiring pre-specification of the number of clusters and
160 of being more repeatable than the highly variable flat method that returns a structured set of clusters
161 [61–63]. However, the linkage criterion selection is critical as it determines how data are combined.
162 Common, linkage criteria include single, complete, average, centroid, Ward's, V (vector), Graph
163 degree. Ward's [64] and average linkage [65] are commonly used in climate analysis [61,62,66–68].
164 In the Ward's method, at each step the pair of clusters that leads to a minimum increase in within-
165 cluster variance is merged together, i.e. total within-cluster variance is minimized. There are some
166 practices using clustering analysis to divide climates for building energy related issues. Wan et al.
167 [51] applied clustering analysis with annual cumulative heat and cold stresses to get 9 clusters for
168 China, and finally dividing 5 bioclimate zones after comparing their similarities. Lau et al. [52] split
169 China into 5 prevailing solar climates using the Ward's method with monthly average daily
170 clearness index. Walsh et al. compared three method, namely the degree-days division, the
171 clustering analysis with climate variables and the administration divisions, for the climate zoning of
172 Nicaragua [43], and proposed an new index the Mean Percentage of Misclassified Areas (MPMA)
173 which shows zoning obtained using the cluster analysis and cooling degree-days may misclassify
174 18% areas, but 30% for the administrative divisions for their case [69].

175

176 **1.2 The Hot Summer and Cold Winter zone (HSCW), China**

177 The Hot Summer and Cold Winter zone in China is used to demonstrate the new method of
178 climate zoning, as the 1.8 million km² area (or 18.8% of China) (Figure 1) is home to ~550 million

179 people, accounts for 48% of China's GDP (2010) [27]. During the period 1995 - 2004 [29] the
180 monthly mean air temperatures (T_{av}) varied between 0 and 10 °C (coldest month) and between 25
181 and 30 °C (hottest month); with $T_{av,day} < 5$ °C for less than 90 days per year and $T_{av,day} > 25$ °C for
182 40 to 110 days per year. However given the historical lack of central heating systems, the indoor
183 conditions in winter are colder than both the Cold and Severe Cold zones [70,71].

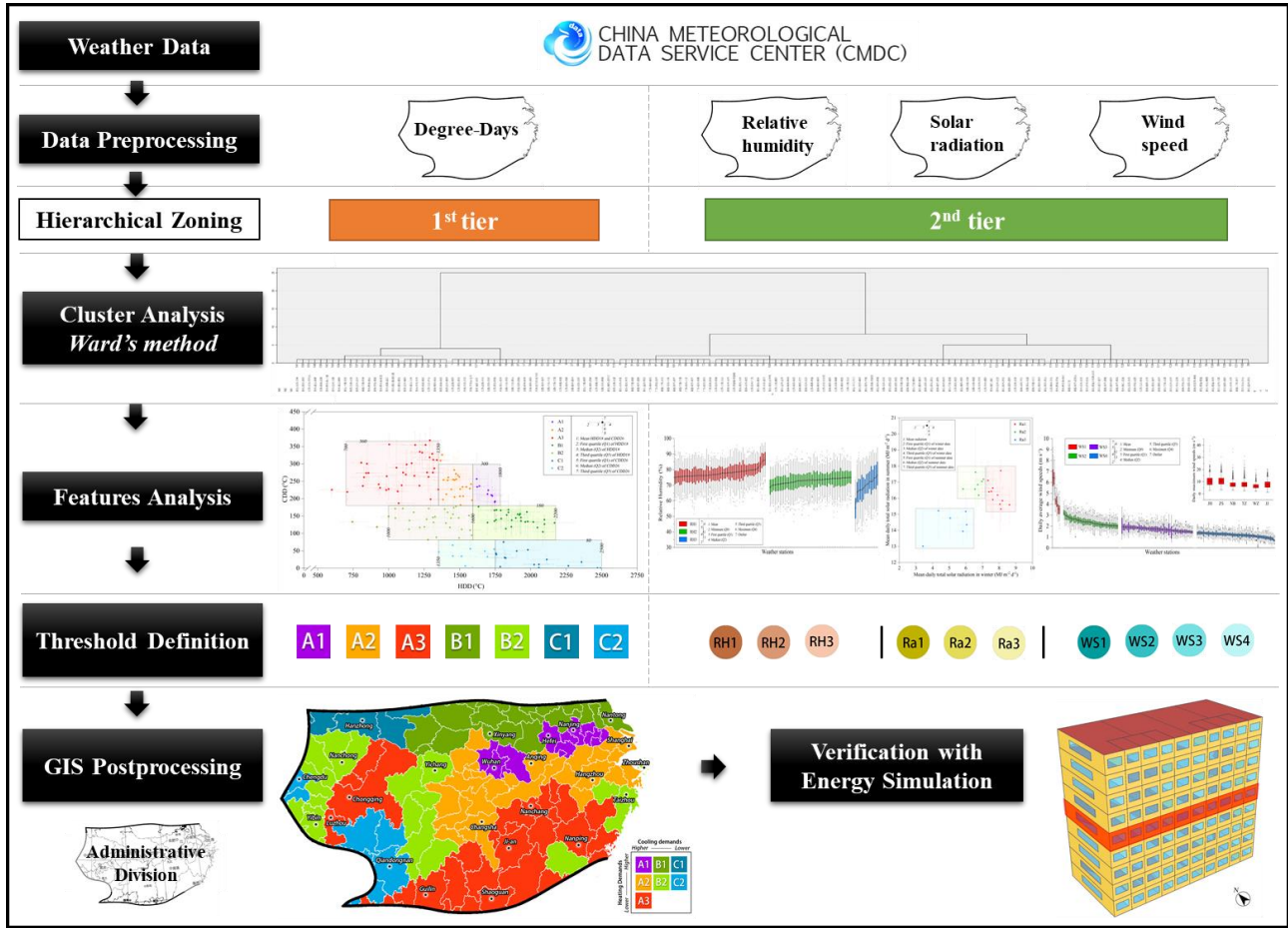
184 The HSCW zone is a transition region with HDD18 (heating degree day based on 18 °C)
185 varying from 700 to 2000 °C. As this wide range is not helpful for climate-responsive passive
186 design strategies, the MOHURD revised national standard (*GB 50176-2016 Code for Thermal*
187 *Design of Civil Building*), sub-divides the zone using HDD18 thresholds (Figure 1b) into 3A (1200
188 - 2000 °C) and 3B (700 - 1200 °C). This is driven by heating demands and building insulation
189 design guidance. As cooling demands, humidity, solar exposure and wind resources are not
190 comprehensively considered it does not provide much practical help to overall climate-responsive
191 passive design [11]. For example, designers would like to know if the wind and outdoor air
192 temperature could enhance natural ventilation and how to balance solar photo-thermal utilization
193 and shading.

194

195 **2 Methods**

196 This research aims to develop a rigorous method of generating finer climate zones for the
197 purpose of building energy design. The Hot Summer and Cold Winter zone of China is used to
198 demonstrate the method, but it could be applied in any region. Figure 2 provides an overview of
199 methods used to subdivide an area.

200



201

202

Figure 2: Overview of the climatic zoning method

203

204 2.1 Data collection and pre-processing

205

206 As climate variations impact energy use in the built environment [72,73] and this region
 207 (middle and lower reaches of the Yangtze River) has experienced increasing temperature for most
 208 cities ($0.3 - 0.4 \text{ } ^\circ\text{C} [10 \text{ y}]^{-1}$) [74], the heating and cooling demands of buildings [58,75] for the
 209 period 2006-2015 are analysed.

210

211 Daily observations from China Meteorological Administration (<http://data.cma.cn/>) [76,77]
 212 weather stations within, and on, the HSCW zone boundary (as defined in the Standard GB 50176-
 213 2016 [29]) are analysed after excluding stations with large amounts of missing data ($>5\%$) and/or
 high elevation stations ($> 1200 \text{ m}$) (Table 2). The stations used are gap-filled by interpolating
 between the two adjacent time periods. The number of stations with missing data is: 16% for wind,

214 6 % for temperature and 12% for relative humidity, with an average (maximum) number of
 215 missing days in the 10-year period: 14 (48), 1 (3) and 2 (7), respectively.

216

217 Table 2: Characteristics of the measurements from state weather stations [78] with the number of stations (N) used

Variable		Height (m)	Range	Resolution	Accuracy	N
Temperature	Daily mean/maximum/minimum	1.50 ± 0.05	-50 - 50 °C	0.1 °C	± 0.2 °C	160
Relative Humidity	Daily mean/minimum	1.50 ± 0.05	0 - 100%	1%	± 4% (≤ 80%) ± 8% (> 80%)	122
Radiation	Daily sunshine hours	---	0 - 24 h	60 s	± 0.1 h	24
	Daily total solar radiation	1.50 ± 0.10	0 - 2000 W m ²	1 W m ²	± 5%	
Wind	Daily mean/maximum wind speed	10 - 12	0 - 60 m s ⁻¹	0.1 m s ⁻¹	± (0.5 m s ⁻¹ +0.03v) v: wind speed (m s ⁻¹)	166
	Direction of maximum	10 - 12	0 - 360 °	3 °	± 5 °	

218

219 Degree-day measures how much warmer or cooler than a base temperature a period is. Here
 220 CDD and HDD are the principal indices used. They are calculated for clustering inputs with base
 221 temperatures of 26 °C for CDD ($T_{B,C}$) and 18 °C for HDD ($T_{B,H}$) from the daily average
 222 temperature (T_i , °C) [29]:

$$223 \quad CDD = \sum_{T_i > T_{B,C}} (T_i - T_{B,C}) \quad (1)$$

$$224 \quad HDD = \sum_{T_i < T_{B,H}} (T_{B,H} - T_i) \quad (2)$$

225 Monthly averages of relative humidity, daily total solar radiation and wind speed are calculated
 226 to analyse the differences in the variables' magnitude and the seasonal variations among selected
 227 stations.

228

229 2.2 Hierarchical agglomerative clustering

230 These data are analysed with hierarchical agglomerative clustering (HAC). Initially, each
 231 station is treated as a separate cluster. These are successively merged using some dissimilarity
 232 between each cluster until the criteria (variance size) to stop merging is reached.

233 To measure the dissimilarity of each variable between any two stations, the squared Euclidean
 234 distance of a variable between station i and j (d_{ij}) is determined:

$$235 \quad d_{ij} = \sum_{t=1}^m (v_{i_t} - v_{j_t})^2 \quad (3)$$

236 where t is the time sequence of each value in a variable dataset of length m , and $v_{i t}$ and $v_{j t}$ are the t^{th}
237 data for station i and station j respectively.

238 In this research, we use the Ward's method for clustering. At each agglomerative step, two
239 clusters with minimum dissimilarity measures are grouped together, then all the dissimilarity
240 measures are updated for the currently available cluster:

$$241 \quad d_{(ij)k} = \frac{n_i+n_k}{n_i+n_j+n_k} d_{ik} + \frac{n_j+n_k}{n_i+n_j+n_k} d_{jk} - \frac{n_k}{n_i+n_j+n_k} d_{ij} \quad (4)$$

242 where $d_{(ij)k}$ is the squared Euclidean distance between the new cluster (ij) and any other cluster k ; d_{ij} ,
243 d_{ik} and d_{jk} are the squared Euclidean distances between clusters as indicated by two subscripts; and
244 n_i , n_j and n_k are the number of stations in each cluster.

245 These results are typically shown in a dendrogram ("Clustering Analysis – Ward's method" in
246 Figure 2).

247

248 **2.3 Analysis and threshold definition**

249 The first tier (Figure 2) of clusters are developed from annual HDD18 and CDD26 data
250 normalized by their respective maxima. The threshold for merging clusters is determined from
251 analysis of the stations HDD18 and CDD26 inter-quartile ranges (IQR, i.e. 75 - 25 percentile). The
252 final map is modified to ensure spatial consistency.

253 In the second tier, the remaining variables (Table 2) are used. For relative humidity, high and
254 low variance areas were identified. The low variance group is sub-divided into extremely high and
255 high humidity. HAC analyses of monthly averages of both daily total solar radiation and wind speed
256 provide two sets of clusters. The seasonal characteristics (especially in summer and winter) of
257 radiation and the magnitudes of the wind speed were evaluated, as references for the specific
258 dividing thresholds.

259

260 **2.4 Verification by energy consumption simulation**

261 To assess the new climate zones, simulations of indoor environment and energy consumption
 262 are performed using EnergyPlus (version 8.4.0, [79]). EnergyPlus is based on the energy balance for
 263 the zone air which considers: I convective internal loads; II convective heat transfer from the zone
 264 surfaces, III heat transfer from inter-zone air mixing, IV heat transfer from infiltration of outside air,
 265 and V the output from mechanical systems providing hot or cold air to the zones to meet heating or
 266 cooling loads [79]:

$$\begin{aligned}
 267 \quad C_z \frac{dT_z}{dt} = & \sum_{i=1}^{N_{sl}} \dot{Q}_i + \sum_{i=1}^{N_{surfaces}} h_i A_i (T_{si} - T_z) + \sum_{i=1}^{N_{zones}} \dot{m}_i C_p (T_{zi} - T_z) + \dot{m}_{inf} C_p (T_{\infty} - T_z) + \dot{Q}_{sys} \\
 268 \quad & \text{I} \qquad \qquad \qquad \text{II} \qquad \qquad \qquad \text{III} \qquad \qquad \qquad \text{IV} \qquad \qquad \qquad \text{V}
 \end{aligned}$$

269 where $C_z \frac{dT_z}{dt}$ is the energy stored in zone air. For more details of the model see [74].

270 The heating and cooling energy consumptions are simulated for a standard Chinese residential
 271 building (Figure 3a) with those construction parameters and occupant's schedule (Table 3) with
 272 weather conditions from representative cities in the different zones. The middle floor of a very
 273 common Chinese megacity medium-rise apartment block [37] (Figure 3a), with a north-south
 274 orientation of the main facades, is simulated. The floor plan (Figure 3b) has four apartments (306
 275 m²) and two stairwells (total 72 m²). Three thermal zones are modelled: the four apartments as a
 276 single zone and the stairwells as two separate zones.

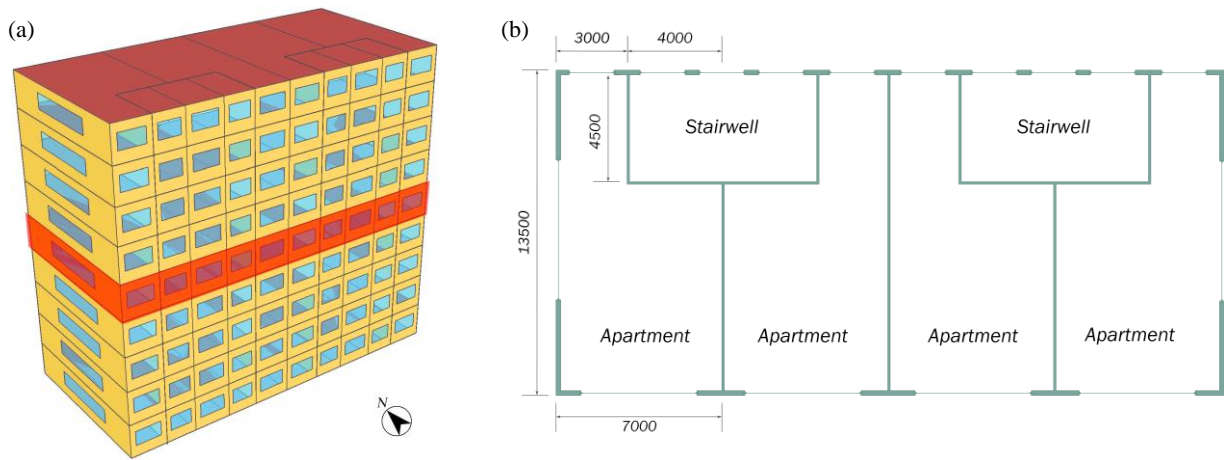
277 These simulations are used to assess the thermal characteristics of this standard building under
 278 different climates and the impact on passive technologies selection, rather than design optimization.
 279 The calculated annual heating/cooling loads are used to access the winter/summer results, and free-
 280 running periods [37] are used in spring and autumn.

282 Table 3: Parameters used in the EnergyPlus simulations are all from [37] (originally refer to the Chinese standard
 283 [27])

Parameters			
U-value (W m ⁻² K ⁻¹)	External wall = 0.804	External window = 2.667 (6 mm coated glazing + 12 mm air + 6 mm clear glazing)	
Window to Wall ratio	North =0.3	South =0.4	East = West =0.2
Air exchange rate (h ⁻¹)	Infiltration = 1	Ventilation =5	
Occupant density (m ⁻²)	0.03 (Activity: sit, heat emission rate: 125.60 W person ⁻¹) (All day occupied)		
Energy consumption index (W m ⁻²)	Lighting = 6.0	Equipment= 4.3	
Thermal comfort range (°C)	18 - 26		

Parameters	
Cooling/Heating mode	Continuously operating when indoor temperature is beyond the thermal comfort range

284



285 Figure 3: EnergyPlus simulations of (a) one floor (red) with (b) floor plan (units: mm, the height of this floor: 2.8
 286 m)

287

288 3 Results and discussion

289 3.1 Subdivision based on Degree-days

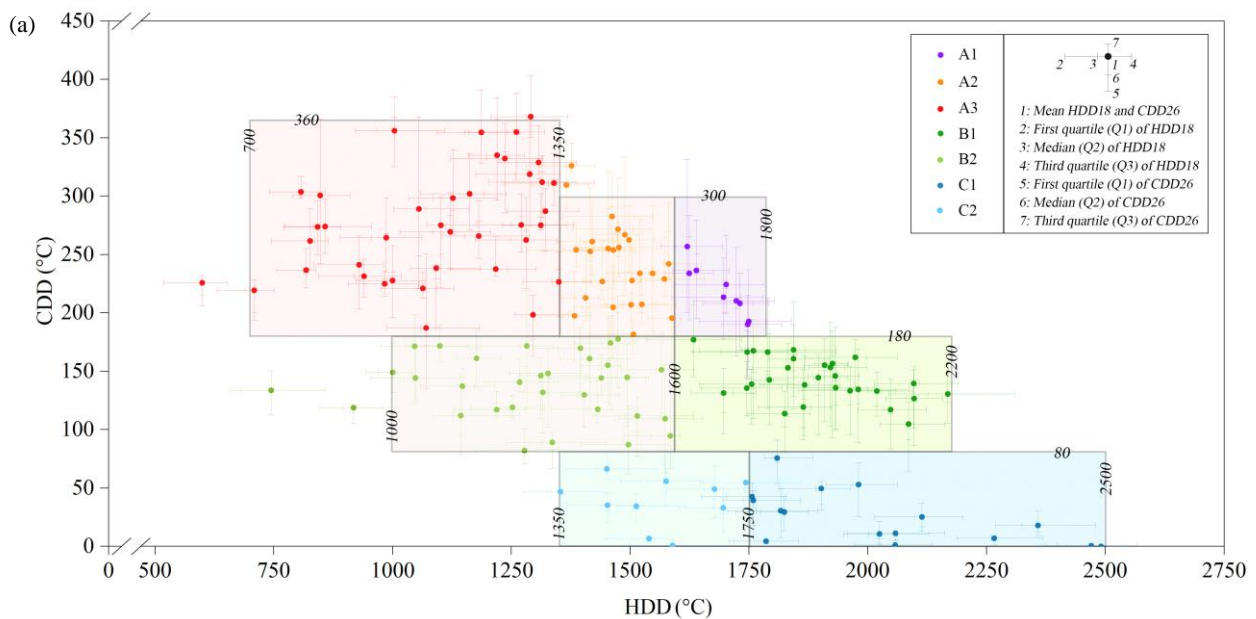
290 Using the methods described in section 2, the HSCW zone is sub-divided into seven (Figure
 291 4). From the CDD26 data three areas with decreasing cooling demands are identified: A (high), B
 292 (medium), C (low). These are sub-divided by heating demands, namely A1, A2, A3, B1, B2, C1 and
 293 C2 (1 for high, 2 for medium and 3 for low). As some stations are on/near the dividing lines (Figure
 294 4a), it is necessary to decide which class they should belong to. Given temporal variations in
 295 temperature may cause some stations to change sub-zone, spatial continuity (Figure 4b) is used to
 296 finalize the selection.

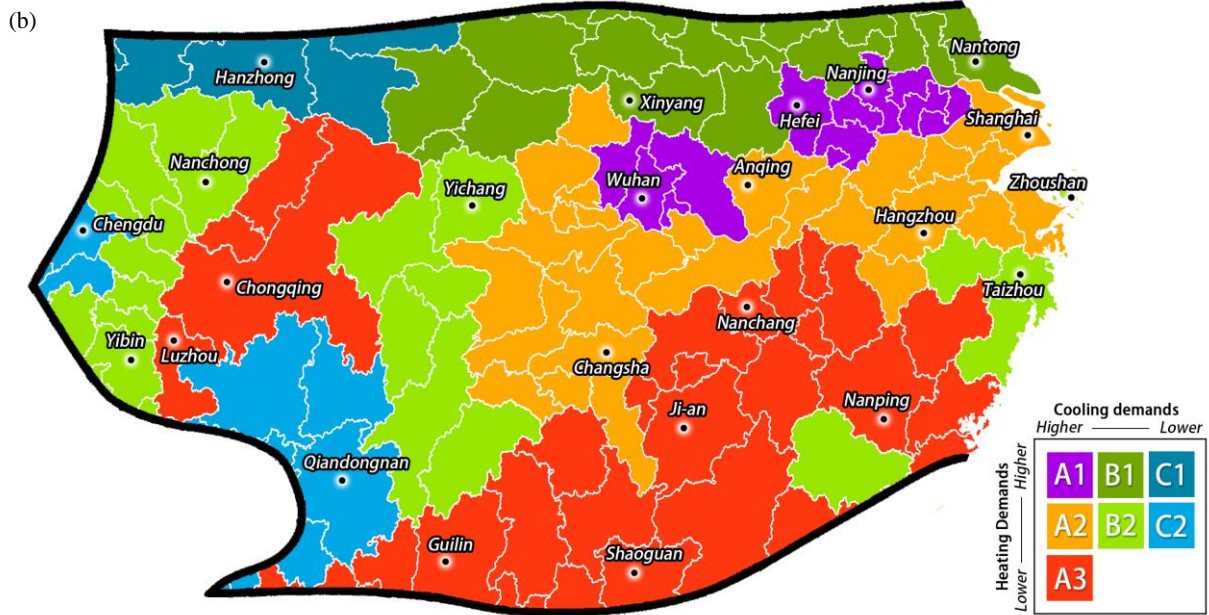
297 Within the HSCW zone, the southeast is obviously warmer than the northwest. The hottest sub-
 298 zone A3 (Figure 4), with the largest cooling demands and lower heating demands, is located along
 299 the southern boundary of the HSCW zone (Jiangxi, south of Hunan, north of Fujian, and northern
 300 part of Guangdong and Guangxi) adjacent to the Hot Summer and Warm Winter (HSWW) zone;
 301 and, in the Sichuan Basin area where mountains surround cities such as Chongqing where air

302 temperatures can reach 42°C [76]. A1 and A2 with the same cooling but larger heating demands (A1
 303 still larger than A2) is in the middle-east of the HSCW zone, downstream of the Yangtze River. It
 304 includes metropolises like Shanghai, Hangzhou, Nanjing, Wuhan, and Changsha. With less cooling
 305 needs B1, B2, C1 and C2 are in the north and west of the HSCW zone, adjacent to the Severe Cold
 306 (SC), Cold (C) and Temperate (T) zones. B1 with large heating demands is to the north. B2 is split
 307 into three: two areas in the west separated by the Chongqing (A2); and, one area on the East China
 308 Sea coast. This area has cooler heatwaves than the surrounding A2 but similar heating requirements.
 309 C1 has higher heating than C2, and they have the lowest cooling needs as it is close to the SC and T
 310 zones.

311 In general, for the HSCW zone: 1) lower latitudes have more cooling demands than higher
 312 latitudes; 2) coastal areas have more cooling needs than inland areas.

313





314 Figure 4: Sub-zones identified using HDD18 and CDD26 (a) mean and quartiles for each observation station with
 315 dividing thresholds and (b) map with city administrative boundaries (white).

316

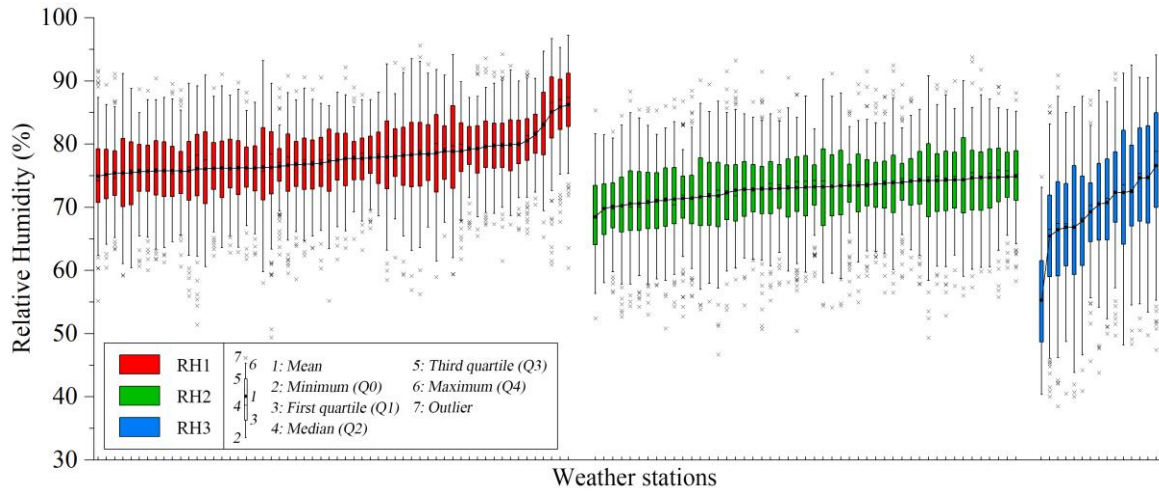
317 **3.2 Second tier zones**

318 Relative humidity is generally high in the HSCW zone, with annual means in most cities of
 319 65% to 85%, and minimum monthly averages above 40% (Figure 5). Given this HVAC energy is
 320 used for dehumidification to secure occupants' comfort. Outdoor temperature and humidity
 321 influence the natural ventilation potential in spring and autumn.

322 The HSCW zone is sub-divided into three relative humidity classes. The three groups differ in
 323 terms of their variability, with the IQR greatest in RH3 (13.5 %) and smaller in RH2 (8.8 %) and
 324 RH1(8.2 %). Overall, the mean is larger in RH1 (annual mean > 75%, minimum monthly average >
 325 60%) than RH2 (annual mean 68 to 75%) and lowest in RH3. Thus, RH1 and RH2 areas experience
 326 uncomfortable or unhealthy (normally < 60% for indoor environments [80]) conditions whereas
 327 RH3 areas will be variable but dry compared to the rest of the HSCW zone.

328

329

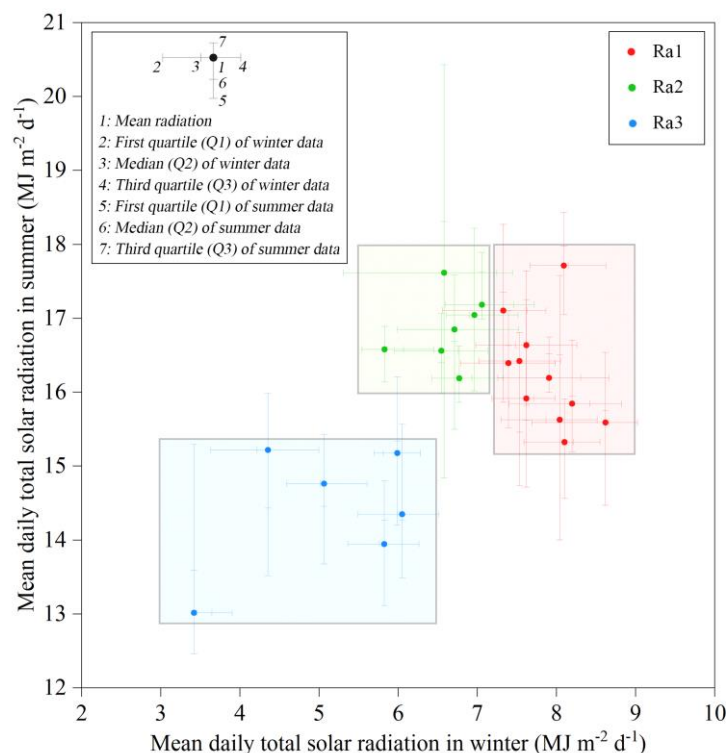


330 Figure 5: Three relative humidity classes (colour) with mean, median and IQR for each station (outlier: > 1.5
331 IQR).

332

333 In winter, direct solar heat gain can improve occupants' thermal comfort and reduce heating
334 demands. However, in summer it can increase the cooling load. HAC analysis of summer and
335 winter daily totals creates three radiation (Ra) clusters (Figure 6): Ra1 - high all year round
336 (summer > 15, winter > 7 MJ·m⁻² d⁻¹); Ra2 - high in summer but lower in winter than Ra1; and Ra3
337 - more limited solar radiation all year round (e.g. summer: 13.02; winter: 3.42 MJ·m⁻² d⁻¹ for the
338 lowest city). Ra3 includes the Sichuan Basin (Chongqing, Chengdu, Luzhou and Mianyang) which
339 is consistent with Lau *et al.*'s five solar zones for China where the Sichuan Basin is a distinct zone
340 [52]. Solar radiation helps solar space heating and domestic hot water production using solar photo-
341 thermal systems [25], and electricity generation using solar photo-electricity [81]. Although
342 applicable for Ra1 and Ra2, there is much less resource in Ra3.

343



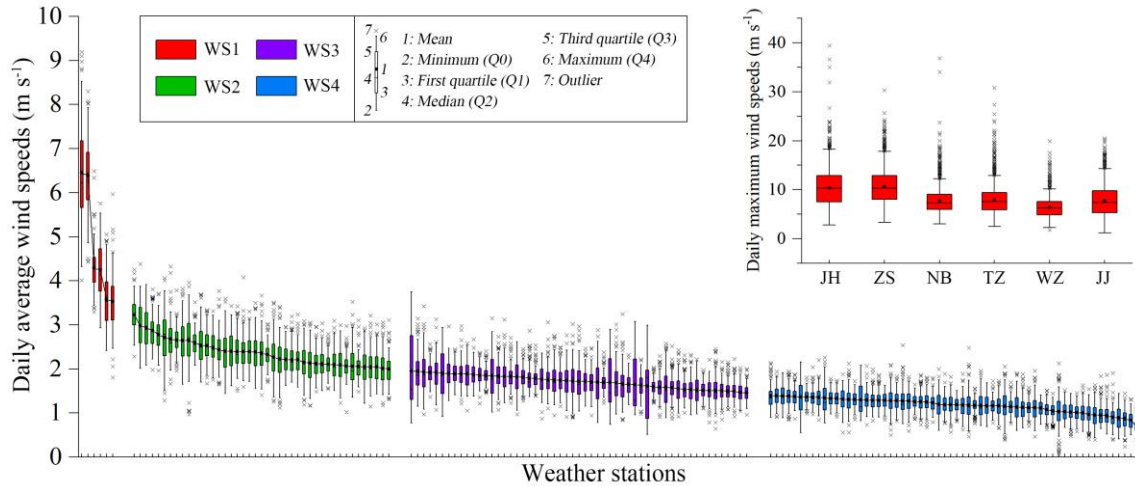
344

345 Figure 6: Three solar radiation classes (colour) derived from HAC analysis of daily total solar radiation in winter
 346 (DJF) and summer (JJA) with each station (mean and quartiles).

347

348 HAC analysis of monthly average wind speeds sub-divided the HSCW into four clusters
 349 (Figure 7) with decreasing mean values: WS1 ($\geq 3.5 \text{ m s}^{-1}$), WS2 ($2.0 \leq \text{WS} < 3.5 \text{ m s}^{-1}$), WS3 (1.5
 350 $\leq \text{WS} < 2.0 \text{ m s}^{-1}$) and WS4 ($< 1.5 \text{ m s}^{-1}$). Higher wind speeds can provide more natural ventilation,
 351 but also induce draughts. Typically, weather stations are in more open places than building sites so
 352 the latter will likely experience much lower wind speeds (e.g. Kent et al. [82]). The highest wind
 353 speeds (WS1) are on the Zhejiang coast an area which experiences tropical depression and
 354 typhoons. Wenzhou has had at least 75 days with daily maximum $\geq 10.8 \text{ m s}^{-1}$ (lower threshold of
 355 tropical depression) in the 10-year period (Figure 7). WS2 covers the Yangtze Plain (middle-lower
 356 reaches of the Yangtze River, near the coast) and a few inland cities; this region has great potential
 357 for natural ventilation. Most of the inland cities in the HSCW zone are classified as WS3 and WS4.
 358 WS3 contains a lot of hilly areas and plateaus, causing higher wind speeds than WS4 are more
 359 sheltered areas.

360



361

362

363

364

365

366

367

368

369

370

371

372

373

374

375

376

377

378

379

380

Figure 7: As Figure 5, but for the four wind classes (colour). The six WS1 cities are left to right: Jinghua (JH), Zhoushan (ZS), Ningbo (NB), Taizhou (TZ), Wenzhou (WZ) and Jiujiang (JJ).

For the full results of sub-zone divisions see Appendix Table A.1.

3.3 Energy simulations for new sub-zones

The impact of the proposed climate sub-zones is assessed using simulations of indoor thermal environment and energy consumption (Section 2.4) for 17 cities that experience the range both first and second tier conditions (Table 4, Figure 4b).

The simulated cooling loads (Table 4, Figure 8) decreased from sub-zone A (mean 82.8 kWh m⁻²) to B (mean 65.3 kWh m⁻²) to C (mean 43.8 kWh m⁻²). The differences in means are assessed using the two independent samples (or two sample Student's) T Test [83]. Between zone A and B, there is a statistically significant difference at an alpha level (α) of 0.05 ($T = 3.741$, $df = 12$, $\text{sig.}(2\text{-tailed}) = 0.003 < \alpha$); and between B and C ($T = 5.863$, $df = 6$, $\text{sig.}(2\text{-tailed}) = 0.001 < \alpha$). The variance within the larger geographical area sub-zone A ($n = 9$, standard deviation (sd) = 11.6 kWh m⁻², IQR = 21.9 kWh m⁻²) is larger than B ($n = 5$, sd = 5.8 kWh m⁻², IQR = 9.9 kWh m⁻²) and C ($n = 3$, sd = 2.9 kWh m⁻², IQR = 2.7 kWh m⁻²).

The average required heating loads of sub-zone A1 is larger than A2 and A3 (cf. 39 to 28 to 13 kWh m⁻²), B1 greater than B2 (cf. 41 to 20 kWh m⁻²), and C1 greater than C2 (44 to 26 kWh m⁻²)

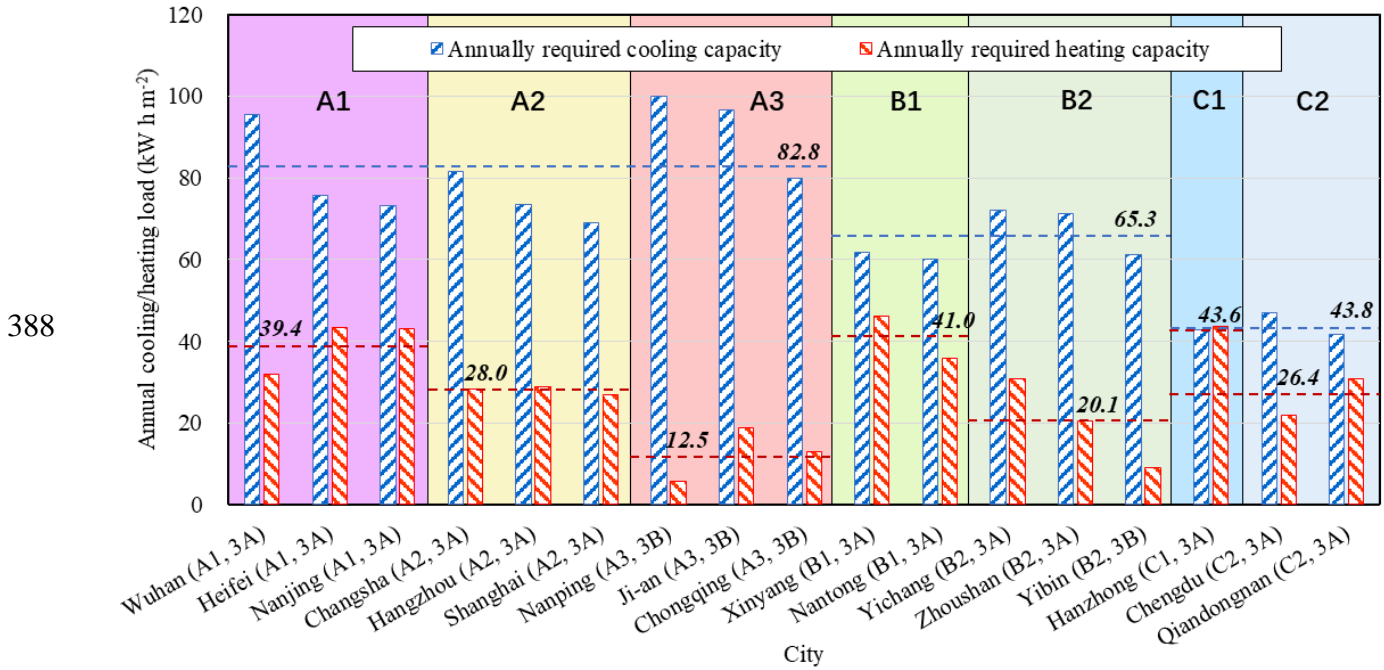
381 (Table 4, Figure 8). Given the small sample sizes (n=1 for C1) no statistical evaluation of difference
 382 is made. The spatial patterns are as expected given the Degree-days based climate zones (Section
 383 3.1).

384

385 Table 4: EnergyPlus simulation (Table 3, Figure 3) results for a typical residential building under different local
 386 weather conditions for 16 representative cities (* missing data required nearest site result assigned).

Sub-zone	Province	City	Humidity	Radiation	Wind	Cooling Load (kWh m ⁻²)	Heating Load (kWh m ⁻²)	Non-heating and cooling period (h)	Mean ± s.d. cooling load
A1	Hubei	Wuhan	RH1	Ra2	WS3	95.5	32.0	3044	82.8 ± 11.6
	Anhui	Hefei	RH2*	Ra1	WS2	75.6	43.3	3192	
	Jiangsu	Nanjing	RH2*	Ra1	WS2	73.1	43.0	3557	
A2	Hunan	Changsha	RH2	Ra2	WS2	81.5	28.2	3271	
	Zhejiang	Hangzhou	RH2	Ra1	WS2	73.6	28.8	3592	
	Shanghai	Shanghai	RH2	Ra1	WS2	68.9	27.0	4067	
A3	Fujian	Nanping	RH1	Ra1	WS4	100.0	5.7	5437	
	Jiangxi	Ji-an	RH1	Ra2*	WS3	96.7	18.8	4869	
	Chongqing	Chongqing	RH1	Ra3	WS4	79.9	12.9	3808	
B1	Henan	Xinyang	RH2	Ra1	WS2	61.9	46.1	4779	65.3 ± 5.8
	Jiangsu	Nantong	RH1	Ra1	WS2	60.1	35.9	5106	
B2	Hubei	Yichang	RH2	Ra3	WS4	72.0	30.7	3354	
	Zhejiang	Zhoushan	RH1	Ra1*	WS1	71.2	20.6	5475	
	Sichuan	Yibin	RH1	Ra3*	WS4	61.3	9.1	4248	
C1	Shanxi	Hanzhong	RH1	Ra2	WS4	42.7	43.6	4833	
C2	Sichuan	Chengdu	RH1	Ra3	WS4	47.1	22.0	4462	
	Guizhou	Qiandongnan	RH1	Ra3*	WS3	41.7	30.8	5237	

387



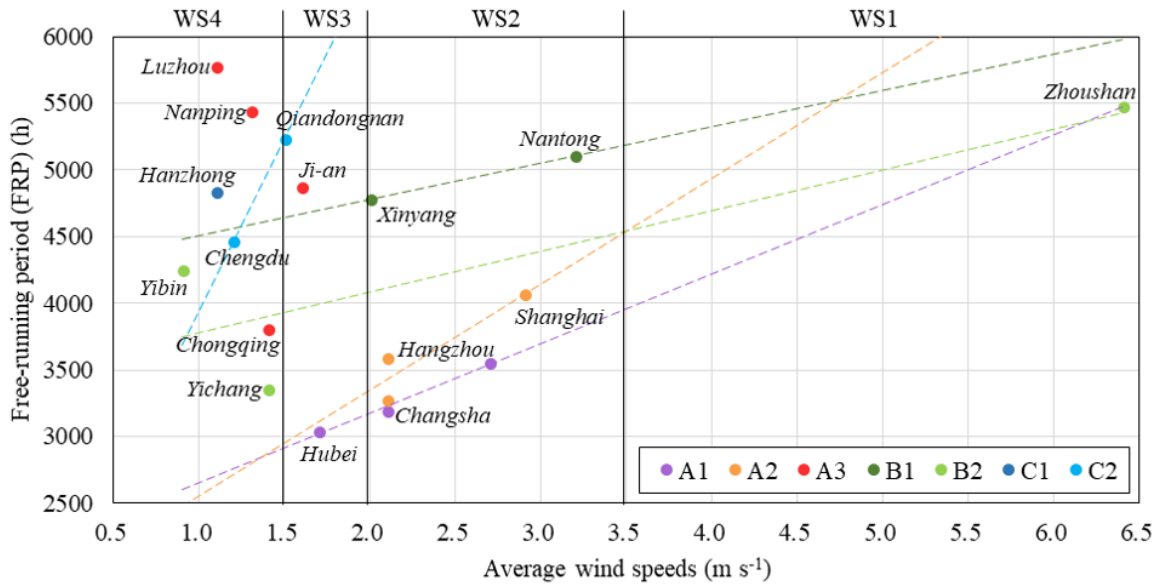
389 Figure 8: Simulated annual cooling and heating loads for a typical building (Figure 3) in 17 representative cities
 390 (Figure 4, Table 4) from new 7 sub-zones (A1, A2, A3, B1, B2, C1 and C2) and current standard divisions
 391 (3A and 3B), and the average for each new sub-zone (indicated above the dash line: blue one shows the
 392 average of cooling load for group A, B and C; red one shows the average of heating load for all sub-zones).

393
 394 Comparing the divisions in current standard [29], among those typical cities, all of three cities
 395 in A3 and one city in B2 belongs to 3B, and all remaining cities belongs to 3A. For cooling loads,
 396 3A is averaged to be 66.5 kWh m⁻² with sd = 15.6 kWh m⁻², and 3B is averaged to be 84.5 kWh m⁻²
 397 with sd = 17.8 kWh m⁻². The discrepancy is not obvious for only two groups available, and their
 398 standard deviations within group are higher than new sub-divisions.

399 The heating load for Nanping is lower than the other A3 cities (Figure 8) as it receives large
 400 amounts of solar radiation all the year round (i.e. Ra1). With means of 8.09 MJ m⁻² d⁻¹ in winter and
 401 17.72 MJ m⁻² d⁻¹ in summer, these are amongst the highest in this region. As indicated, the external
 402 heat gains from solar radiation can significantly reduce the need for additional heating.

403 The free-running period (FRP) when neither heating nor cooling is required (i.e. in spring and
 404 autumn) can be extended with appropriate shading and natural ventilation [37]. As higher wind
 405 speeds can enhance natural ventilation in transition seasons, the relations between the length of this
 406 period and wind sub-zones (stratified by temperature zone) are analysed (Figure 9). Areas with

407 higher wind speeds tend to have the longer simulated FRP: for A1 $FRP_{WS2} > FRP_{WS3}$; for B2
 408 $FRP_{WS1} > FRP_{WS4}$; and C2, $FRP_{WS3} > FRP_{WS4}$. However, as expected A3 does not follow this
 409 pattern because of the many other factors that influence the length of the FRP.
 410



411
 412 Figure 9: The relation between average wind speed and simulated length of a period not needing heating or
 413 cooling (h), comparison among wind classes (Figure 7) for cities (dots) in thermal sub-zones (A1, A2, A3,
 414 B1, B2, C1, C2). The tendency (dashed lines) follows that the larger wind speed contributes to the longer
 415 free-running period for A1, A2, B1, B2 and C2.
 416

417 4 Conclusions

418 A new method to obtain zones for climate-responsive building design for heating and cooling
 419 based on hierarchical agglomerative clustering (HAC) with a technique to generalise threshold
 420 criteria is presented. The method is demonstrated for the Chinese Hot Summer and Cold Winter
 421 zone, which is regarded as a challenging region for low-carbon heating and cooling solutions given
 422 its diverse climate. The impact of climate zoning on energy consumption is demonstrated by
 423 simulating (EnergyPlus) heating and cooling loads for a typical residential building in different sub-
 424 zones. The cooling demands across sub-zones (A, B and C) are significantly different with mean
 425 heating demands also different ($A1 > A2 > A3$; $B1 > B2$; $C1 > C2$). Areas with higher wind speeds

426 can potentially have longer free-running periods.

427 The main conclusions from this study are:

- 428 • The two-tier method of climate zoning based on first HDD and CDD, and secondly
429 relative humidity, solar radiation and wind speed provides more consistent climate sub-
430 zones. These will enhance the implementation of the improved climate-responsive passive
431 design in practice. The method will help the identification of key climatic factors that will
432 affect the building energy design and the utilisation of natural resources.
- 433 • The current standard with two sub-zones for the Hot Summer and Cold Winter zone does
434 not properly identify the diverse climates in this region, so would likely result in the
435 poorer energy efficiency of building designs. Sub-division into seven, based on heating
436 and cooling, improves the spatial resolution of heating/cooling loads. These are
437 demonstrated (by simulation) to have different building energy demands. This is a useful
438 reference for the policy/building code makers for heating and cooling strategies of this
439 region.
- 440 • The method could be applied to any other regions. Weather station data used provide
441 insight for areas but any specific site.

442

443 **Acknowledgement**

444 The research work is based on the UK-China collaborative research project ‘Low carbon
445 climate-responsive Heating and Cooling of Cities (LoHCool)’ supported by the National Natural
446 Science Foundation of China [NSFC Grant No. 51561135002] and the UK Engineering and
447 Physical Sciences Research Council [EPSRC Grant No. EP/N009797/1]. The research is associated
448 with the China National Key R&D Programme ‘Solutions to Heating and Cooling of Buildings in
449 the Yangtze River Region’ [Grant No: 2016YFC0700300]. Mr Jie Xiong would like to thank the
450 China Scholarship Council for its financial support as a sponsored researcher at the University of
451 Reading [Grant No: 201706050009] and Miss Xingxing Wu for her assistant in weather data
452 collection.

453

454 **References**

- 455 [1] Intergovernmental Panel on Climate Change. Climate Change 2013: The Physical Science Basis.
456 Cambridge: Cambridge University Press; 2013.
- 457 [2] Crowley TJ. Causes of Climate Change Over the Past 1000 Years. *Science* (80-) 2000;289:270–7.
458 doi:10.1126/science.289.5477.270.
- 459 [3] Qu W, Xu L, Qu G, Yan Z, Wang J. The impact of energy consumption on environment and public
460 health in China. *Nat Hazards* 2017;87:675–97. doi:10.1007/s11069-017-2787-5.
- 461 [4] Rafindadi AA, Yusof Z, Zaman K, Kyophilavong P, Akhmat G. The relationship between air
462 pollution, fossil fuel energy consumption, and water resources in the panel of selected Asia-Pacific countries.
463 *Environ Sci Pollut Res* 2014;21:11395–400. doi:10.1007/s11356-014-3095-1.
- 464 [5] ChinaDaily. Full text of President Xi’s speech at opening ceremony of Paris climate summit 2015.
465 http://africa.chinadaily.com.cn/2015-12/01/content_22592476.htm (accessed March 15, 2018).
- 466 [6] EU. Directive 2010/31/EU of the European Parliament and of the Council of 19 May 2010 on the
467 energy performance of buildings. *Off J Eur Union* 2010;L153:13–35.
- 468 [7] Building energy conservation research center of Tsinghua University. Annual Research Report on
469 the Development of Building Energy Conservation in China 2017. Beijing: China Architecture & Building
470 Press; 2017.
- 471 [8] Yao R, Steemers K, Li B. Introduction to sustainable urban and architectural design. *Introd. to*
472 *Sustain. Urban Archit. Des.*, Beijing: China Architecture and Building Press; 2006.
- 473 [9] Lam JC, Wan KKW, Tsang CL, Yang L. Building energy efficiency in different climates. *Energy*
474 *Convers Manag* 2008;49:2354–66. doi:10.1016/j.enconman.2008.01.013.
- 475 [10] Cai Z, Yin Y, Wennerstern R. From energy efficiency to integrated sustainability in housing
476 development in China: a case study in a hot-summer/cold-winter zone in China. *J Hous Built Environ*
477 2013;28:329–44. doi:10.1007/s10901-012-9316-3.
- 478 [11] Feng Y. Thermal design standards for energy efficiency of residential buildings in hot
479 summer/cold winter zones. *Energy Build* 2004;36:1309–12. doi:10.1016/j.enbuild.2003.08.003.
- 480 [12] Schnieders J, Feist W, Rongen L. Passive Houses for different climate zones. *Energy Build*
481 2015;105:71–87. doi:10.1016/j.enbuild.2015.07.032.
- 482 [13] Krarti M, Ihm P. Evaluation of net-zero energy residential buildings in the MENA region. *Sustain*
483 *Cities Soc* 2016;22:116–25. doi:10.1016/j.scs.2016.02.007.
- 484 [14] Gaglia AG, Tsikaloudaki AG, Laskos CM, Dialynas EN, Argiriou AA. The impact of the energy
485 performance regulations’ updated on the construction technology, economics and energy aspects of new
486 residential buildings: The case of Greece. *Energy Build* 2017;155:225–37. doi:10.1016/j.enbuild.2017.09.008.
- 487 [15] Özkan DB, Onan C. Optimization of insulation thickness for different glazing areas in buildings
488 for various climatic regions in Turkey. *Appl Energy* 2011;88:1331–42. doi:10.1016/j.apenergy.2010.10.025.
- 489 [16] Yang L, Lam JC, Tsang CL. Energy performance of building envelopes in different climate zones
490 in China. *Appl Energy* 2008;85:800–17. doi:10.1016/j.apenergy.2007.11.002.
- 491 [17] Wang Y, Chen Y, Zhou J. Dynamic modeling of the ventilated double skin façade in hot summer
492 and cold winter zone in China. *Build Environ J* 2016;106:365–77.

493 doi:<http://dx.doi.org/10.1016/j.buildenv.2016.07.012>.

494 [18] Jaber S, Ajib S. Thermal and economic windows design for different climate zones. *Energy Build*

495 2011;43:3208–15. doi:10.1016/j.enbuild.2011.08.019.

496 [19] Hamdaoui S, Mahdaoui M, Allouhi A, El Alaiji R, Kousksou T, El Bouardi A. Energy demand and

497 environmental impact of various construction scenarios of an office building in Morocco. *J Clean Prod*

498 2018;188:113–24. doi:10.1016/j.jclepro.2018.03.298.

499 [20] Yao R, Li B, Steemers K, Short A. Assessing the natural ventilation cooling potential of office

500 buildings in different climate zones in China. *Renew Energy* 2009;34:2697–705.

501 doi:10.1016/j.renene.2009.05.015.

502 [21] Li Y, Li X. Natural ventilation potential of high-rise residential buildings in northern China using

503 coupling thermal and airflow simulations. *Build Simul* 2015;8:51–64. doi:10.1007/s12273-014-0188-1.

504 [22] Tan Z, Deng X. Assessment of Natural Ventilation Potential for Residential Buildings across

505 Different Climate Zones in Australia. *Atmosphere (Basel)* 2017;8:1–17. doi:10.3390/atmos8090177.

506 [23] Babaizadeh H, Haghghi N, Asadi S, Broun R, Riley D. Life cycle assessment of exterior window

507 shadings in residential buildings in different climate zones. *Build Environ* 2015;90:168–77.

508 doi:10.1016/j.buildenv.2015.03.038.

509 [24] Singh R, Lazarus IJ, Kishore VVN. Uncertainty and sensitivity analyses of energy and visual

510 performances of office building with external venetian blind shading in hot-dry climate. *Appl Energy*

511 2016;184:155–70. doi:10.1016/j.apenergy.2016.10.007.

512 [25] He Z. Chinese national standards for application of solar thermal technology in civil buildings.

513 *Energy Procedia* 2015;70:347–52. doi:10.1016/j.egypro.2015.02.133.

514 [26] The Ministry of Housing and Urban-Rural Development of the People’s Republic of China. GB

515 50189-2005 Design standard for energy efficiency of public buildings. Beijing: China Architecture & Building

516 Press; 2005.

517 [27] The Ministry of Housing and Urban-Rural Development of the People’s Republic of China. JGJ

518 134-2010 Design standard for energy efficiency of residential buildings in hot summer and cold winter zone.

519 Beijing: China Architecture & Building Press; 2010.

520 [28] Ministère de l’Environnement de l’Énergie et de la Mer. Réglementation Thermique 2012. 2012.

521 [29] The Ministry of Housing and Urban-Rural Development of the People’s Republic of China. GB

522 50176-2016 Code for thermal design of civil building. Beijing: China Architecture & Building Press; 2016.

523 [30] The Ministry of Housing and Urban-Rural Development of the People’s Republic of China. GB

524 50176-93 Thermal design code for civil building. Beijing: China Planning Press; 1993.

525 [31] ASHRAE. ANSI/ASHRAE Standard 169-2013 Climatic Data for Building Design Standards.

526 Atlanta: ASHRAE; 2013.

527 [32] California Energy Commission. California Energy Maps - California Building Climate Zone Areas

528 2015. http://www.energy.ca.gov/maps/renewable/building_climate_zones.html (accessed November 15, 2017).

529 [33] Hall VT, Deter ER. California climate zone descriptions for new buildings. Sacramento,

530 California: California Energy Commission; 1995.

531 [34] Australia Building Codes Board. NCC 2016 Building Code of Australia - Volume One. Canberra:

532 Australia Building Codes Board; 2016.

533 [35] Department of the Environment and Energy. Nation House Energy Rating Scheme - Climate Zone

534 Map 2012. http://www.nathers.gov.au/sites/all/themes/custom/nathers_2016/climate-map/index.html (accessed

535 March 16, 2017).

536 [36] NatHERS National Administrator. Nationwide House Energy Rating Scheme (NatHERS) -
537 Software Accreditation Protocol. 2012.

538 [37] Yao R, Costanzo V, Li X, Zhang Q, Li B. The effect of passive measures on thermal comfort and
539 energy conservation. A case study of the hot summer and cold winter climate in the Yangtze River region. *J*
540 *Build Eng* 2018;15:298–310. doi:10.1016/j.job.2017.11.012.

541 [38] Givoni B. *Man, Climate and Architecture*. 2nd ed. London: Applied Science Publishers; 1969.

542 [39] Jacobeit J. Classifications in climate research. *Phys Chem Earth* 2010;35:411–21.
543 doi:10.1016/j.pce.2009.11.010.

544 [40] Köppen W. *Die Klimate der Erde (Climates of the Earth)*. Berlin: 1923.

545 [41] Kottek M, Grieser J, Beck C, Rudolf B, Rubel F. World map of the Koppen-Geiger climate
546 classification updated. *Meteorol Zeitschrift* 2006;15:259–63. doi:10.1127/0941-2948/2006/0130.

547 [42] Olgyay V. *Design with Climate: Bioclimatic Approach to Architectural Regionalism*. Princeton:
548 Princeton University Press; 2015.

549 [43] Walsh A, Cóstola D, Labaki LC. Comparison of three climatic zoning methodologies for building
550 energy efficiency applications. *Energy Build* 2017;146:111–21. doi:10.1016/j.enbuild.2017.04.044.

551 [44] Institute for Building Environment and Energy Conservation. Regional classification according to
552 judgment criteria of housing industry 2013. <http://ees.ibec.or.jp/documents/> (accessed July 16, 2017).

553 [45] Bureau of Energy Efficiency. *Energy Conservation Building Code User Guide*. New Delhi: Bureau
554 of Energy Efficiency; 2013.

555 [46] Ali S, Sharma M, Maiteya V. Climatic classification for building design in India. *Archit Sci Rev*
556 1993;36:31–4. doi:https://doi.org/10.1080/00038628.1993.9696730.

557 [47] Spanish Ministry of Public Service. Documento Básico DB-HE Ahorro de Energía. Código
558 Técnico la Edif., 2013, p. 67137–209.

559 [48] de la Flor FJS, Lissén JMS, Domínguez SÁ. A new methodology towards determining building
560 performance under modified outdoor conditions. *Build Environ* 2006;41:1231–8.
561 doi:10.1016/j.buildenv.2005.05.035.

562 [49] Salmerón JM, Álvarez S, Molina JL, Ruiz A, Sánchez FJ. Tightening the energy consumptions of
563 buildings depending on their typology and on Climate Severity Indexes. *Energy Build* 2013;58:372–7.
564 doi:10.1016/j.enbuild.2012.09.039.

565 [50] Agence Nationale pour le Developpement des Energies Renouvelables et de l’Efficacite
566 Energetique Maroc. Les éléments techniques du projet de la réglementation thermique du bâtiment au Maroc.
567 2011.

568 [51] Wan KKW, Li DHW, Yang L, Lam JC. Climate classifications and building energy use
569 implications in China. *Energy Build* 2010;42:1463–71. doi:10.1016/j.enbuild.2010.03.016.

570 [52] Lau CCS, Lam JC, Yang L. Climate classification and passive solar design implications in China.
571 *Energy Convers Manag* 2015;48:2006–15. doi:10.1016/j.enconman.2007.01.004.

572 [53] Walsh A, Cóstola D, Labaki LC. Review of methods for climatic zoning for building energy
573 efficiency programs. *Build Environ* 2017;112:337–50. doi:10.1016/j.buildenv.2016.11.046.

574 [54] The Chartered Institution of Building Services Engineers. *Degree-days: Theory and Application*.
575 London: The Chartered Institution of Building Services Engineers; 2006.

576 [55] Bessec M, Fouquau J. The non-linear link between electricity consumption and temperature in

577 Europe: A threshold panel approach. *Energy Econ* 2008;30:2705–21. doi:10.1016/j.eneco.2008.02.003.

578 [56] Dash PK, Gupta NC, Rawat R, Pant PC. A novel climate classification criterion based on the

579 performance of solar photovoltaic technologies. *Sol Energy* 2017;144:392–8.

580 doi:10.1016/j.solener.2017.01.046.

581 [57] Ministerio de Fomento e IDAE. *Fundamentos Te'cnicos de la Calificacio'n Energe'tica de*

582 *Viviendas*. Centro de Publicaciones Secretari'a General Te'cnica Ministerio de Fomento; 1999.

583 [58] Verichev K, Carpio M. Climatic zoning for building construction in a temperate climate of Chile.

584 *Sustain Cities Soc* 2018;40:352–64. doi:10.1016/j.scs.2018.04.020.

585 [59] Jain AK, Murty MN, Flynn PJ. Data clustering: a review. *ACM Comput Surv* 1999;31:264–323.

586 doi:10.1145/331499.331504.

587 [60] Mahajan M, Nimbhorkar P, Varadarajan K. The planar k-means problem is NP-hard. *Theor*

588 *Comput Sci* 2012;442:13–21. doi:10.1016/j.tcs.2010.05.034.

589 [61] Fovell RG, Fovell M-YC. Climate Zones of the Conterminous United States Defined Using

590 Cluster Analysis. *J Clim* 1993;6:2103–35. doi:10.1175/1520-0442(1993)006<2103:CZOTCU>2.0.CO;2.

591 [62] Dezfuli AK. Spatio-temporal variability of seasonal rainfall in western equatorial Africa. *Theor*

592 *Appl Climatol* 2011;104:57–69. doi:10.1007/s00704-010-0321-8.

593 [63] Manning CD, Raghavan P, Schutze H. *An Introduction to Information Retrieval*. Inf Retr Boston

594 2009:1–18. doi:10.1109/LPT.2009.2020494.

595 [64] Ward JH. Hierarchical Grouping to Optimize an Objective Function. *J Am Stat Assoc*

596 1963;58:236–44. doi:10.1093/comjnl/26.4.354.

597 [65] Murtagh F. A Survey of Recent Advances in Hierarchical Clustering Algorithms. *Comput J*

598 1983;26:354–9.

599 [66] Badr HS, Zaitchik BF, Dezfuli AK. A tool for hierarchical climate regionalization. *Earth Sci*

600 *Informatics* 2015;8:949–58. doi:10.1007/s12145-015-0221-7.

601 [67] Baeriswyl P -a., Rebetez M. Regionalization of precipitation in Switzerland by means of principal

602 component analysis. *Theor Appl Climatol* 1997;58:31–41. doi:10.1007/BF00867430.

603 [68] Gong X, Richman MB. On the Application of Cluster Analysis to Growing Season Precipitation

604 Data in North America East of the Rockies. *J Clim* 1995;8:897–931. doi:10.1175/1520-

605 0442(1995)008<0897:OTAOCA>2.0.CO;2.

606 [69] Walsh A, Cóstola D, Chebel L. Performance-based validation of climatic zoning for building

607 energy e ffi ciency applications. *Appl Energy* 2018;212:416–27. doi:10.1016/j.apenergy.2017.12.044.

608 [70] Li B, Du C, Yao R, Yu W, Costanzo V. Indoor thermal environments in Chinese residential

609 buildings responding to the diversity of climates. *Appl Therm Eng* 2018;129:693–708.

610 doi:10.1016/j.applthermaleng.2017.10.072.

611 [71] Cao B, Luo M, Li M, Zhu Y. Too cold or too warm? A winter thermal comfort study in different

612 climate zones in China. *Energy Build* 2016;133:469–77. doi:10.1016/j.enbuild.2016.09.050.

613 [72] Li DHW, Yang L, Lam JC. Impact of climate change on energy use in the built environment in

614 different climate zones - A review. *Energy* 2012;42:103–12. doi:10.1016/j.energy.2012.03.044.

615 [73] Cao J, Li M, Wang M, Xiong M, Meng F. Effects of climate change on outdoor meteorological

616 parameters for building energy-saving design in the different climate zones of China. *Energy Build*

617 2017;146:65–72. doi:10.1016/j.enbuild.2017.04.045.

618 [74] Shi P, Sun S, Wang M, Li N, Wang J, Jin Y, et al. Climate change regionalization in China (1961-

619 2010). *Sci China Earth Sci* 2014;57:2676–89. doi:10.1007/s11430-014-4889-1.

620 [75] Erba S, Causone F, Armani R. The effect of weather datasets on building energy simulation

621 outputs. *Energy Procedia* 2017;134:545–54. doi:10.1016/j.egypro.2017.09.561.

622 [76] China Meteorological Administration. Dataset of Daily Surface Observation Data in China. China

623 Meteorol Data Serv Cent n.d.

624 http://data.cma.cn/data/cdcdetail/dataCode/SURF_CLI_CHN_MUL_DAY_V3.0.html (accessed July 1, 2017).

625 [77] China Meteorological Administration. Dataset of Daily Solor Radiation in China. China Meteorol

626 Data Serv Cent n.d. http://data.cma.cn/data/cdcdetail/dataCode/RADI_MUL_CHN_DAY.html (accessed July 1,

627 2017).

628 [78] General Administration of Quality Supervision Inspection and Quarantine of the People’s Republic

629 of China (AQSIQ). GB/T 35221-2017 Specifications for surface meteorological observation - General. Beijing:

630 Standards Press of China; 2017.

631 [79] U.S. Dept. of Energy. EnergyPlus™ Version 8.4.0 Documentation - Engineering Reference. 2016.

632 [80] Chartered Institution of Building Services, Engineers (CIBSE). CIBSE Guide A: Environmental

633 design. Norfolk: Page Bros. (Norwich) Ltd.; 2015.

634 [81] Li Y, Zhang G, Lv GZ, Zhang AN, Wang RZ. Performance study of a solar photovoltaic air

635 conditioner in the hot summer and cold winter zone. *Sol Energy* 2015;117:167–79.

636 doi:10.1016/j.solener.2015.04.015.

637 [82] Kent CW, Lee K, Ward HC, Hong J-W, Hong J, Gatey D, et al. Aerodynamic roughness variation

638 with vegetation: analysis in a suburban neighbourhood and a city park. *Urban Ecosyst* 2018;21:227–243.

639 doi:<https://doi.org/10.1007/s11252-017-0710-1>.

640 [83] Heumann C, Schomaker M, Shalabh. Introduction to Statistics and Data Analysis. 1st ed. Basel:

641 Springer International Publishing; 2016.

642

643 **Appendix**

644 Table A.1: Sub-zones for building energy efficiency in the Hot Summer and Cold Winter zone of China

Province	City	WMO reference	Latitude (°E)	Longitude (°N)	Altitude (m)	Sub-zone	Humidity	Radiation	Wind
Shanghai	Shanghai	58362	121.27	31.24	5.5	A2	RH2	Ra1	WS2
Chongqing	Chongqing	57516	106.28	29.35	259.1	A3	RH1	Ra3	WS4
Hubei	Wuhan	57494	114.03	30.36	23.6	A1	RH1	Ra2	WS3
Hubei	Yichang	57461	111.22	30.44	133.1	B2	RH2	Ra3	WS4
Hunan	Changsha	57687	112.55	28.13	68	A2	RH2	Ra2	WS2
Hunan	Hengyang	57874	112.24	26.25	116.6	A3	RH2	Ra2	WS3
Hunan	Xiangxi	57649	109.41	28.14	208.4	B2	RH1	Ra3	WS4
Jiangxi	Nanchang	58606	115.55	28.36	46.9	A3	RH2	Ra2	WS3
Jiangxi	Ji-an	57799	114.55	27.03	71.2	A3	RH1	Ra2	WS3
Jiangxi	Ganzhou	57993	115	25.52	137.5	A3	RH2	Ra2	WS4
Anhui	Hefei	58321	117.18	31.47	27	A1	RH2	Ra1	WS2

Province	City	WMO reference	Latitude (°E)	Longitude (°N)	Altitude (m)	Sub-zone	Humidity	Radiation	Wind
Anhui	Fuyang	58203	115.44	32.52	32.7	B1	RH3	Ra1*	WS2
Anhui	Huangshan	58531	118.17	29.43	142.7	A2	RH1	Ra1	WS3
Zhejiang	Hangzhou	58457	120.1	30.14	41.7	A2	RH2	Ra1	WS2
Zhejiang	Taizhou	58665	121.25	28.37	4.6	B2	RH2	Ra1	WS1
Zhejiang	Zhoushan	58477	122.06	30.02	35.7	B2	RH1	Ra1*	WS1
Sichuan	Chengdu	56187	103.52	30.45	547.7	C2	RH1	Ra3	WS4
Sichuan	Yibin	56492	104.36	28.48	340.8	B2	RH1	Ra3*	WS4
Sichuan	Mianyang	56196	104.44	31.27	522.7	B2	RH1*	Ra3	WS3
Sichuan	Luzhou	57608	105.26	28.1	377.5	A3	RH1	Ra3	WS4
Guizhou	Zhunyi	57606	106.5	28.08	972	C2	RH1	Ra3*	WS3
Guizhou	Qiandongnan	57832	108.4	26.58	626.9	C2	RH1	Ra3*	WS3
Jiangsu	Nanjing	58238	118.54	31.56	35.2	A1	RH2*	Ra1	WS2
Jiangsu	Nantong	58265	121.36	32.04	3.6	B1	RH1	Ra1	WS2
Henan	Xinyang	58208	115.37	32.1	42.9	B1	RH2	Ra1	WS2
Henan	Nanyang	57178	112.29	33.06	129.2	B1	RH3	Ra1	WS3
Fujian	Nanping	58737	118.19	27.03	154.9	A3	RH1	Ra1	WS4
Fujian	Ningde	58846	119.31	26.4	32.4	A3	RH2*	Ra1*	WS3
Shanxi	Hanzhong	57127	107.02	33.04	509.5	C1	RH1	Ra2*	WS4
Shanxi	Ankang	57245	109.02	32.43	290.8	C1	RH2	Ra2	WS4
Guangxi	Guilin	57957	110.18	25.19	164.4	A3	RH2	Ra2	WS2

645

Description of characteristics			
	Highest relative humidity High relative humidity Lower and variable relative humidity	High solar radiation all year High solar radiation in summer Low solar radiation all year	Higher wind speed High wind speed Medium wind speed Low wind speed
	* Data are unavailable for this station, classification results obtained from nearest station		

646